Cyclicity in multivariate time series and applications to functional MRI data

Yuliy Baryshnikov and Emily Schlaffly

***Abstract*— One of the challenging problems in fMRI data analysis is the absence of natural time scale at which to consider the traces of the *resting state*, the aggregate name for the processes in the brain happening in the absence of task of strong external stimuli. This necessitates development of the tools that are able to extract from the time series information invariant with respect to reparametrization of the time coordinate. A recently developed notion of *cyclicity*, based on the hierarchy of *iterated path integrals* and corresponding algorithms were applied to several hundreds of the fMRI records, to reveal potential presence of an external auditory stimulus.**

I. Introduction

This paper explores applications of *cyclicity*, a novel approach to understanding a class of phenomena that are cyclic but not periodic, to the neurophysiological data, specifically to recovering cyclic patterns in the resting state, or *default state*.

A. Cyclicity and Periodicity

The distinction between the *cyclic* and *periodic* phenomena is important. Periodicity of a process does imply cyclicity, but not vice versa – there are plenty of processes that are manifestly cyclic, but not periodic, in the sense that no time interval, i.e. *period* P can be found such that shift of the process along the time axis by P leaves it invariant. Examples of cyclic yet not periodic processes include cardiac cycle; muscle-skeletal complex movements exercised during a gait; population dynamics in closed ecosystems; business cycles and many others. It is natural also to look for cyclic phenomena in the mental activity.

The predominant focus on the periodic processes can be explained by the availability of powerful tools exploiting harmonic analysis (Fourier or Laplace transforms, etc). The intrinsic limitation of these tools stems from the fact that they rely on the structure of the time as a *homogenous space*; without this structure, the natural bases for the decompositions underlying harmonic analysis in all its flavours just do not exist.

This work aims at the introduction of several interconnected computational tools for understanding cyclic phenomena, which are explicitly reparametrization invariant. While we outline the key results and algorithms underlying this techniques, the complete presentation of the cyclicity toolbox will be addressed elsewhere [1]

This work was supported by ONR (N00014-11-1-017) and AFOSR (FA9550-10-1-05678).

Y. Baryshnikov is Professor of Mathematics and Electrical and Computer Engineering, University of Illinois at Urbana-Champaign, 1409 W. Green Street Urbana, IL 61801, USA ymb@illinois.edu

E. Schlaffly is with the Dapertment of Mathematics, University of Illinois at Urbana-Champaign, 1409 W. Green Street Urbana, IL 61801, USA

B. Dynamic Functional Connectivity Problem

We start with a brief overview of the dynamic functional connectivity problem.

Dynamic patterns of functional connectivity present several challenges to data analysis, especially for the problem of the resting state connectivity.

Until quite recently, the sampling rate of the brain activity signals was low, and the data comparatively noisy that led to (tacit) assumption that there is little dynamical changes in the signal interrelationships within the measurement window.

While this assumption allowed to discover and start analizing the global patterns of interdependencies of brain regions, reflecting the brain functionality, it was clearly preventing understanding of the causal dependences between the processes running in the different parts of the brain.

The so-called "resting state" of the brain, customarily associated with self-consciousness, the processes of mind not triggered by some external stimuli are one of the most exciting paradigms of the modern neurophysiology. The emergence of functional magnetic resonance imaging, tracking the levels of oxygen carried to the brain cells as a proxy for the activity signals, became the de facto standard of the resting state studies, see [7]. It is not surprising therefore, that in an attempt to understand the spatio-temporal patterns of brain activity in the resting states, the researchers turned to tools allowing more granularity in the time domain. Most of the work in the area pursued rather traditional venues of time series analysis (correlations, information theory based metrics), somewhat limiting the resulting analysis (compare [2], [8]).

While the underlying drivers and models for the resting state activities remain one of the key challenges, empirical studies allowed to identify several intrinsic connectivity networks.

The prevalent techniques of detecting dynamics patterns in fMRI traces are relying heavily on some apriori filtering, such as the sliding window analysis [9]. Despite several successes, these methods suffer from heavy dependency of the results on the parameters of the smoothening procedure: too short a window fails to suppress the noise enough, and too long a window risks filtering out the actual dynamics of the resting state processes, characteristic frequencies of which are still not characterized.

At this background, the techniques that are explicitly designed to be time-reparametrization invariant, are ideally

suited for analysis of the processes without a base frequency, or aperiodic, if cyclic. Recovery of the intrinsic connectivity networks should be significantly enhanced by such tools.

This short note outlines some first results towards this goal. Here is the content breakdown: Section II describes the general difference between periodic and cyclic processes, and introduces the necessary notation. Section III describes the key tool, reparametrization invariant *path integrals*, while Section IV deals with reinterpretation of the first nontrivial path integrals, algebraic areas of 2D projections, in terms of cyclic orderings, the theme continued in Section V. The applications to fMRI data are contained in Section VI.

C. Acknowledgements

Conversations with Prof. Fatima Husain (UIUC) on the neurophysiological aspects of the problem are gratefully acknowledged.

II. Phenomena Cyclic and Periodic

The problem outlined above, of uncovering the presumed dynamic patterns of default functional connectivity network is one of many problems dealing with analysis of phenomena that are cyclic yet not periodic.

In common language, the notions of being cyclic and periodic are often used interchangeably, and for a reason: any cyclic phenomenon, that is the one whose underlying state space is a circle $\mathbf{C} \cong \mathbb{S}^1$, can be lifted to a periodic phenomenon on the state space $\mathbf{T} \cong \mathbb{R}^1$ which is the natural covering of $\mathbf{C}$. The domain and the range of the mapping $\mathcal{T} : \mathbf{T} \to \mathbf{C}$ can be parameterized in a consistent way, so that any two points in $\mathbf{T}$ separated by the *period* P are mapped into the same point of $\mathbf{C}$. Equivalently, this amounts to the representation of the circle $\mathbf{C} \cong \mathbb{R}/P\mathbb{Z}$.

We will be referring to any such parameter on $\mathbf{C}$ as the *internal clock*, and the consistent parametrization on $\mathbf{T}$ as the *internal time*, reserving for the points of $\mathbf{C}$ the name *internal state*.

Just by definition, a cyclic phenomenon is periodic, if represented as a function of its internal time. Obviously, such a parametrization is not unique: if t is the parameter on $\mathbb{R}$ such that $\mathcal{T}(t) \equiv \mathcal{T}(t+P)$, then any reparametrization (i.e. a continuous one-o-one mapping) $t = s + \phi(s)$, where ϕ is a P-periodic, will have the same property.

However, the observed, *measured* phenomena are normally parameterized not by the their internal clocks: they are parameterized by the time. The internal clocks do not necessarily coincide with the the time progression, not even after a linear reparametrization. In general, if the internal clock cannot be represented as a sum of a linear and a periodic function of the time, the cyclic phenomena cannot be made periodic by *any* reparametrization.

The implications of this absence of a periodic (in they *physical time*) representation of a cyclic phenomenon are important. For periodic phenomena a powerful mathematical tool – Fourier analysis (and its numerous versions, Laplace, cosine etc transforms, operator calculus, ...) – is readily available. However, it depends critically on the structure of the time space as a homogeneous space of the groups of shifts. The fact that the (*abelian*) group of shifts acts on the timeline, leaving the law of the observable functions invariant means that these functions admit a representation as a linear combination of the characters of the group of the shifts of time, that is eigenfunctions of the shift operator, thus exponential functions,

All of these mechanisms are absent in the case of cyclic but non-periodic functions, and a new conceptual foundation for recovering and understanding *cyclicity* without relying on the periodicity is needed. In this note we will present an approach towards this goal.

A. Reparametrization

Consider an arbitrary parametrization of the internal clock,

$$R : \mathbb{R}^1 \to \mathbf{T}, \tag{1}$$

which we will be interpreting as the evolution of the internal clock under the physical time: $R(\tau) \in \mathbf{T}$ is the state of the internal clock at time τ.

A P-periodic function $f : \mathbf{T} \to V$ with values in some range V (i.e. a cyclic phenomenon) defines unambiguously a function on the internal state space $f : \mathbf{C} \to V$. The composition $f \circ R : \tau \mapsto f(R(\tau)) \in V$ is the *cyclic phenomenon observed at time* τ.

We remark that one should not confuse the cyclicity with quasi-periodicity: quasi-periodicity of a function means that it is obtain from a function on a torus via pull back of a affine immersion of the real line, thus again, relying on the group structures.

A natural proposal to recover the underlying periodic function f on the internal clock space from observations of $f \circ R$ is to identify the *values* taken by the observables thus recovering the internal state space. A version of this idea is to single out special values of $f \circ R$, for example the critical points of some linear functional of the data.

Unfortunately, this procedure is very fragile and easily disrupted by noise of the observations.

III. Trajectories and Their Invariants

From now on, we will assume that the range of the observed processes is a d-dimensional Euclidean space $V \cong \mathbb{R}^d$, with coordinates $x_j, j = 1, \dots d$. Before attacking the specific problem, of recovering the cyclic nature of the observed processes, we will address the general question, of *reparametrization invariant functionals of trajectories*: what are the functions of trajectories that do not depend on how one traverses them?

This question is classical, and has an answer in terms of the iterated path integrals, a theory going back to Picard and Riemann, but rigorously reintroduced into the modern mathematical practice by K.-T. Chen.

A. Iterated Integrals

Iterated integrals are explicitly reparamatrization invariant functionals of a trajectory γ. They are defined in an inductive fashion.

Definition 3.1: Iterated integrals of order zero are just constants, associating to any trajectory γ a number $I(\gamma) \equiv c, c \in \mathbb{R}$. For $k > 0$, the iterated integrals of order k are defined as the vector space generated by the functionals

$$I(\gamma) := \sum_{1 \leqslant j \leqslant d} \int_{t_s}^{t_f} I_j(\gamma_{t_s,t}) d\gamma_j(t), \tag{2}$$

where I_j are the iterated integrals of order $< k$.

1) Examples: Iterated Integrals of Low Orders: It is immediate that the invariants of order 1 are exactly the increments of the trajectory over the interval I,

$$I_k(\gamma) = \gamma_k(t_f) - \gamma_k t_s.$$

Starting at order 2, the iterated integrals render more information than mere increments. By definition, the iterated integrals of order 2 are spanned by the functionals

$$I_{k,l} = \int_{t_s}^{t_f} \gamma_k(t) d\gamma_l(s). \tag{3}$$

In other words, the iterated integrals of order 2 are spanned by the (algebraic) areas under the projections of the trajectory γ onto various coordinate 2-planes.

2) Completeness of the Iterated Integrals: From the construction of the iterated integrals it is immediate that they are invariant with respect to a reparametrization. Also, it is clear that a parallel translation $\gamma \mapsto \gamma + \mathbf{c}, \mathbf{c} \in V$ leaves the iterated integrals invariant.

We will call a *detour* a segment of the trajectory γ that is backtracked immediately. In other words, if the trajectory γ can be represented as a concatenation

$$\gamma = \gamma_1 | \gamma_2 | \gamma_2^{-1} | \gamma_3,$$

(where | denotes concatenation of the trajectories, such that the endpoint of one corresponds to the starting point of the other, and γ^{-1} is the trajectory γ traversed backward), then the segment

$$\gamma_2 | \gamma_2^{-1}$$

is a detour.

It can be seen easily by an inductive argument, that removing a detour does not change any of the iterated integrals.

We will be calling a trajectory without detours *irreducible*. A generic perturbation of a curve makes it irreducible.

The fundamental result of [3] states that the *iterated path integrals* form a full system of the invariants of irreducible trajectories (defined up to reparametrization) in Euclidean space, up to a translation of the curve:

Theorem 3.2 ([3]): Two irreducible trajectories

$$\gamma_1, \gamma_2 : I \to V$$

are equal up to translation and reparametrization if and only if all their corresponding iterated integrals coincide.

IV. Leaders and Followers

Completeness of the system of functionals on the trajectories in V given by iterated integrals suggests that any data-driven exploration *of parametrization-independent features* can rely on these functionals as a rich enough tool.

We apply this idea to the quest of recovery of cyclic phenomena. One of the frequent features of a cyclic phenomena is a self-sustained cycling, in which an active process activates another process, and proceed through a cyclic sequence of such activation-relaxation instances. (Examples of such self-sustained dynamics are the trophic chains; virtuous cycles in innovation dynamics, such as software-hardware coupling; autocatalytic chains[6] etc.)

Staying within model-free the data analysis paradigm, we aim to capture the visually evident *leader-follower* relationship as seen on Figure 1.

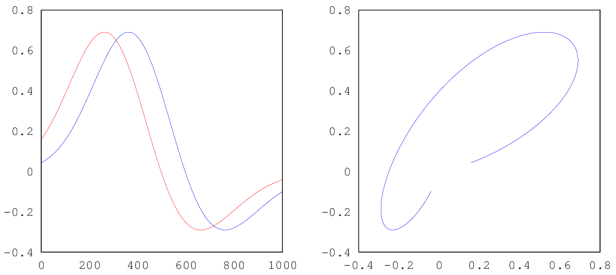

Fig. 1: Leader follower relation we would like to capture. Plotting the functions shown on the left against each other produces a curve encircling a positive oriented area (on the right).

The key observation is the following: if one effect precedes another, the *oriented area* on the parametric joint plot of the corresponding functions will surround a *positive algebraic area*. Of course, the semantics of this assumes that k and l are consubstantial; if their nature is antagonistic, the lead-follow relation flips.

We take this consideration as our primitive on which to build the procedures of data analysis.

A. Lead matrix

Let us start with the situation when the trajectory γ is closed.

Consider the iterated integrals

$$A_{kl} := \frac{1}{2} \int_t \gamma_l d\gamma_k - \gamma_k d\gamma_l. \tag{4}$$

Clearly, these integrals are equal to the oriented areas of the two-dimensional projections of the trajectory γ on the coordinate planes.

Definition 4.1: The skew-symmetric matrix

$$A = (A_{kl})_{1 \leqslant k,l \leqslant J}$$

is called the *lead matrix*.

An interpretation of the lead matrix coefficients therefore can be that an element A_{kl} is positive if l *follows* k.

B. Lead Matrix with Noisy Data

To be able to use the lead matrix in applications, one needs some statistical guarantees of its recoverability from noisy observation,

$$\boldsymbol{\gamma}^{\epsilon}(\tau) = \boldsymbol{\gamma}(\tau) + \boldsymbol{\epsilon}(\tau), \tag{5}$$

where $f : \mathbf{C} \to V$ is the cyclic observable; R the internal clock parametrization, $\boldsymbol{\gamma}(\tau) = f(R(\tau))$, and $\boldsymbol{\epsilon} : \mathbb{R} \to V$ the noise.

It should be noted that a naive procedure of taking the sampled lead matrix with coefficients

$$(A(\boldsymbol{\gamma}^{\epsilon}_{a,b}))_{kl} := \frac{1}{2}\int_a^b \boldsymbol{\gamma}^{\epsilon}_k(t)d\boldsymbol{\gamma}^{\epsilon}_l(t) - \boldsymbol{\gamma}^{\epsilon}_l(t)d\boldsymbol{\gamma}^{\epsilon}_k(t) \tag{6}$$

and averaging over time, setting

$$\hat{A} := \lim_{t\to\infty} \frac{1}{t} A(\boldsymbol{\gamma}^{\epsilon}_{0,t}), \tag{7}$$

would fail already for the noise being multidimensional Brownian motion (or some stationary version thereof, like the Ornstein-Uhlenbeck process) for the following reason: the algebraic area of the planar Brownian motion scales as t over the intervals of length t (see, e.g. [5]), adding a nonvanishing error in the limit, and making $\hat{A}$ an inconsistent statistics for the lead matrix.

Still, a modification of the procedure can overcome this difficulty.

We make the following (rather lax) assumptions:

- the *one period lead matrix* with coefficients

$$(A^p)_{kl} := \frac{1}{2}\int_{\mathbf{C}} f_k df_l - f_l df_k \tag{8}$$

  is nonzero;
- the clock parametrization $R : \mathbb{R} \to \mathbf{T}$ has positive asymptotic speed:

$$\liminf_{s,t,t-s\to\infty} \frac{R(t) - R(s)}{t - s} > 0;$$

- the noise process is Markov,
- centered,

$$\mathbb{E}\boldsymbol{\epsilon}(t) - \boldsymbol{\epsilon}(s) \equiv 0;$$

- the algebraic areas of the noise process are well-defined, centered,

$$\mathbb{E}A(\boldsymbol{\epsilon}_{s,t}) \equiv 0;$$

  and have at most linearly growing variance,

$$\mathbb{V}A(\boldsymbol{\epsilon}_{s,t}) \leqslant C(t - s).$$

We remark that the Brownian motions or Ornstein-Uhlenbeck processes satisfy these assumptions.

Let $l_1, l_2, l_3, \ldots$ a sequence of the interval lengths, such that

$$l_k \to \infty; l_k/L_k = 0,$$

where $L_k = \sum_{j\leqslant k} l_j$.

Definition 4.2: Define the *partitioned* sampled lead matrices (corresponding to the sequence $l_1, l_2, \ldots$) as

$$\bar{A}^{\epsilon}(k) = \frac{1}{L_k}\sum_{j\leqslant k} A(\boldsymbol{\gamma}^{\epsilon}_{L_{j-1},L_j}), \tag{9}$$

(that is the sum of sampled lead matrices over the consecutive intervals of lengths $l_1, l_2, \ldots$).

Theorem 4.3: The normalized sampled lead matrices converge to the normalized lead matrix over one period,

$$\bar{A}^{\epsilon}(k)/\parallel \bar{A}^{\epsilon}(k) \parallel \to A^p/\parallel A^p \parallel \tag{10}$$

This law of large numbers proves the consistency of the partitioned sample lead matrices estimator in our model.

V. Chain of Offsets Model

Consider now the situation where the components of the trajectory $\boldsymbol{\gamma}$ are quintessentially equivalent processes, with the coordinated internal clocks, but run with a system of offsets. Again, such a system is what one would expect in a process where internally similar subsystems cyclically excite each other.

Such a system would engender a collection of offsets $\alpha_j \in \mathbb{S}^1$, (defined up to a shift). We assume that these processes essentially track the same underlying function, ϕ, with, perhaps, some rescaling. That means that

$$f_k(t) = a_k\phi(t - \alpha_j), \tag{11}$$

(in terms of the internal clock), while the (noise-less trajectory) is given by

$$\boldsymbol{\gamma}_k(\tau) = a_k\phi(R(\tau) - \alpha_k), k = 1, \ldots, d. \tag{12}$$

From now on we will assume this *chain of offsets model* (COOM). (The notion of cyclic (non-periodic) processes is of course much broader, and other models will necessarily emerge to address situations not adequately described by the COOM.)

For now, the central question we will address, is whether under COOM, one can discover the *cyclic order* of the functions f_j, or, equivalently, the cyclic order of $\alpha_j, j = 1, \ldots, d$ by recovering from the (perhaps, noisy version) of the trajectory, $\boldsymbol{\gamma}^{\epsilon}$, the sampled lead matrix.

We start by computing the lead matrix over the period under COOM.

Expand the primary function ϕ (defined on circle $\mathbf{C}$ parameterized by the internal clock $\mathbf{T}$) into the Fourier series,

$$\phi(T) = \sum c_k \exp(2\pi i k T). \tag{13}$$

Lemma 5.1: The lead matrix over period A^p is given by

$$A(\phi) = 2\pi a_k a_l \left(\sum_{m\geqslant 1} m|c_m|^2 \sin(m(\alpha_k - \alpha_l))\right)_{k,l} \tag{14}$$

(Proof is an easy computation.)

A. Recovering the offsets

Now, given the skew-symmetric matrix A approximating the lead matrix over one period A^p, one might try to reconstruct the cyclic ordering of the offset phases α_k's, $k = 1, \ldots, d$. We describe here two algorithms for this recovery.

1) Low Rank Approximation: A natural simplifying assumption, not infrequent in practice, stipulates that the Fourier expansion (13) is dominated by the leading coefficient: when $|c_1|^2$ much larger that $\sum_{|k|\geqslant 2} |c_k|^2$ (we ignore the constant term, as it is irrelevant to the cyclic behavior).

If ϕ has just a single harmonic in its expansion, then the skew symmetric matrix A^p would have rank two (spanned by the two rank one matrices, $A^{\pm}$, with

$$A^{+}_{kl} = a_k a_l \sin(\alpha_k)\cos(\alpha_l)$$

and

$$A^{-}_{kl} = a_k a_l \cos(\alpha_k)\sin(\alpha_l).$$

In general, even if the function ϕ is not harmonic, and the observations are noisy, one still can expect, if the sampled lead matrix approximates the one period lead matrix well, and the leading harmonic is dominating ϕ, that $\bar{A}$ is well approximated (in Frobenius norm) by the *rank 2 matrix*

$$P\bar{A}P,$$

where P is the projection on the 2-plane spanned by the eigenvectors corresponding to the largest in absolute value purely imaginary eigenvalues.

Furthermore, it is immediate that the corresponding (complex conjugated) eigenvectors of this rank 2 matrix are given by

$$v_1 = e^{i\psi}\left(e^{2\pi i\alpha_1}, e^{2\pi i\alpha_2}, \ldots, e^{2\pi i\alpha_J}\right), v_2 = \bar{v}_1$$

(for some phase ψ).

Taking the SVD of A_1 and the arguments of the components of the first eigenvector would then produce the desire cyclic order.

2) Using MCMC: Another approach to try to find a collection of harmonic functions

$$\xi_j(t) = \sin(t - \alpha_j)$$

is to start with a random collection of unit vectors $\mathbf{r} = \{r_k \in \mathbf{C}\}_{k=1,\ldots,J}\}$, and run a MCMC process, perturbing the elements of the collection one by one, and accepting a small perturbation if the induced matrix $A^{\mathbf{r}}$ has better correlation with the lead matrix A we wish to reproduce. In other words, one replaces $\mathbf{r}_1$ with $\mathbf{r}_2$ if

$$\mathtt{tr}(A^{\mathbf{r}_1}A^{\top}) < \mathtt{tr}(A^{\mathbf{r}_2}A^{\top}).$$

VI. Applying Cyclicity

A. Artificial data

We start with noiseless data: we generated $J = 12$ traces of harmonic functions $\sin(t-\alpha_k)$ with random phase offsets (cyclically ordered), and sampled them, at 625 samples for period for 16 periods. The results are shown on Figure 2. We can see the banded, nearly cyclic lead matrix, the spectrum having just two nontrivial (complex conjugated) eigenvalues, and the components of the leading eigenvector close to the circle of radius $1/\sqrt{J}$.

Next, consider a similar example, adding to each of the samples an *iid* normally distributed value with SNR $\sigma \approx 1.42$

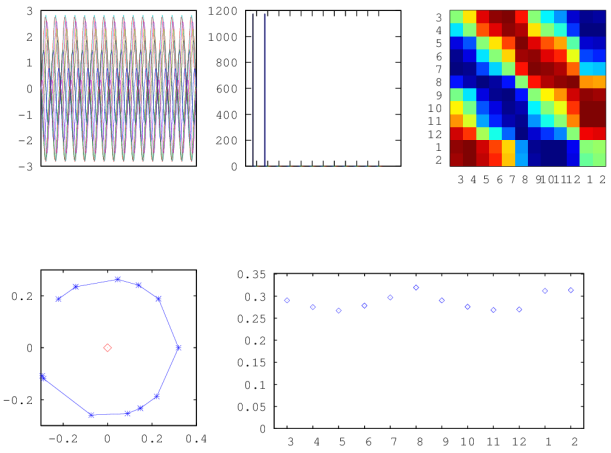

Fig. 2: Top row left: traces of the observations; middle: absolute values of the eigenvalues of the lead matrix; right: lead matrix (reordered according to the cyclic order of the phases of the eigenvectors of the lead matrix). Bottom row left: the components of the eigenvector; right: their absolute values, ordered according to the order of their arguments.

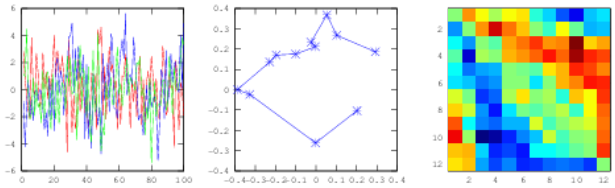

Fig. 3: Explanations of the plots are given on the caption of Fig. 2.

(Figure 3). As one can imagine, the sample is quite noisy: the spectral separation of the leading eigenvalue is far smaller; the realigned lead matrix is not so apparently circular and the components of the leading eigenvector do not align on a circle. Still, the cyclic ordering (in this case, the identity permutation) is recovered remarkably well.

B. Analysis of Human Connectome Project Data

To test the cyclicity-based approach on the fMRI data we turned to Human Connectome Project[1], a large consortium of research centers, based at the Washington University in St. Louis, aiming at aggregating high quality annotated data of brain scanning aimed at the recovery of the patterns of connectivity in human brain.

In this study, we pulled the fMRI traces of resting subjects.

The 200 traces obtained are resting-state fMRI scans available directly from the HCP website[2] or using the Amazon S3 server[3]. Once downloaded, the nifti files (.nii.gz) can be further processed for use in Matlab using packages available from Mathworks.

[1] `http://www.humanconnectomeproject.org/`

[2] `https://db.humanconnectome.org/data/projects/HCP_900`

[3] Credentials should be obtained from the website and then a program like Cyberduck can be used to browse the HCP directory.

The subjects were scanned using a customized Siemens 3T "Connectome Skyra" at Washington University in St. Louis Missouri using the following parameters:

- Repetition time (TR): 720 ms
- Voxel dimension:$2 \times 2 \times 2$ mm
- Frames per run: 1200 (total run duration = 14:33)

The scans that we downloaded have been preprocessed to remove distortions and register the data to standard MNI coordinate space.

The subjects themselves are "healthy adults, ages 22-35, whose race/ethnicity is representative of the US population."[4]

A variety of additional information is recorded for each subject including, for example, measures of alertness, cognition, and sensory functions (audition is measured using a Words in Noise test and all subjects with this parameter recorded have scores between -2.0 and 14.0 on a scale of -2.0 to 26.0 with lower scores indicative of better performance).

For each of the subjects, the data were then aggregated into 33 voxel groups, the ROIs, corresponfding to anatomically identified regions of the brain, often with a function, or a group of functions correlated with it.

For each of the subjects, the full cyclicity analysis was run, yileding a collection of lead matrices (33×33 skew-symmetric matrices); the implied cyclic permutations and and vectors of the amplitudes of the components of the leading eigenvalues, serving as a proxy for the signal strength, as discussed above.

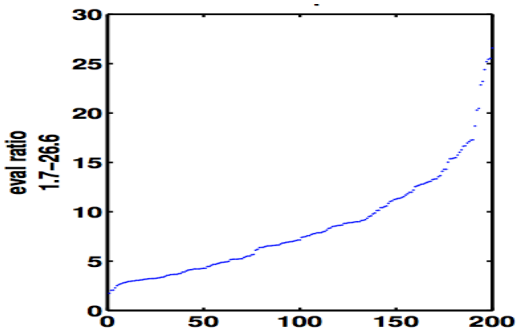

Fig. 4: Cumulative distribution of the number of subjects with the ratio of the leading and next in size absolute values of the eigenvalues.

1) Eigenvalue Ratios: The predictive power of the leading eigenvector in describing the cyclic structure of the ROIs in the time series can be deduced, heuristically, from the ratio of the absolute value of the leading eigenvalue over the larges of the absolute values of the remaining components: if the reordered absolute values are $|\lambda_1| = |\lambda_2| > |\lambda_3| = |\lambda_4| > \ldots$, then the quality of the ordering defined by the components of u_1 is $|\lambda_1|/|\lambda_3|$.

For the trajectories whose components are *iid* Brownian bridges, it is easy to show that in the limit of large number of regions, the ratio is close to 2 [1]. Any data with higher ratio point to rejection of such a hypothesis.

[4] http://humanconnectome.org/data/

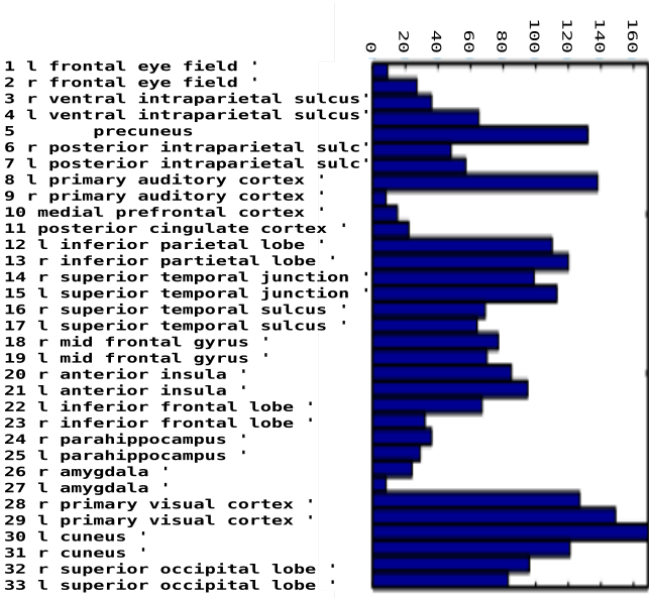

Fig. 5: Histogram of top 12 regions (highest phase magnitude) for 200 HCP subjects.

Figure 4 shows the cumulative histogram of the ratios $|\lambda_1|/|\lambda_3|$. The data point at the presence of strong signal.

2) Active regions: Our goal in this study was to understand whether there exist some common cyclic process, a consiousness pattern, that can be detected in a large number of the subjects.

To this end, we first identified the group of ROIs exhibiting high signal. The plot on Figure 5 shows the numbers of subjects for which the corresponding region was amongst the top 12, in terms of the amplitude of the corresponding component of the top eigenvector fo the lead matrix.

This week we analyzed the data from the 200 HCP subjects and compared the top n regions in each subject ($n \in \{5, 8, 12\}$). We then summarized the results by histogramming the number of appearances of each roi for all 200 of the subjects. The results for $n = 12$ are shown in 5. These results were then used to generate the following groups of 10 most pronounced ROIs:

Group 1	
30	l cuneus
29	l primary visual cortex
08	l primary auditory cortex
05	precuneus
28	r primary visual cortex
31	r cuneus
13	l ventral intraparietal sulcus*
15	l posterior intraparietal sulc*
12	r ventral intraparietal sulcus*
14	r posterior intraparietal sulc*

Functionally, these regions are given by

- *Ventral intraparietal sulcus (VIPS)*: visual attention and saccadic eye movement
- *Posterior (caudal) IPS*: perception of depth from stereopsis

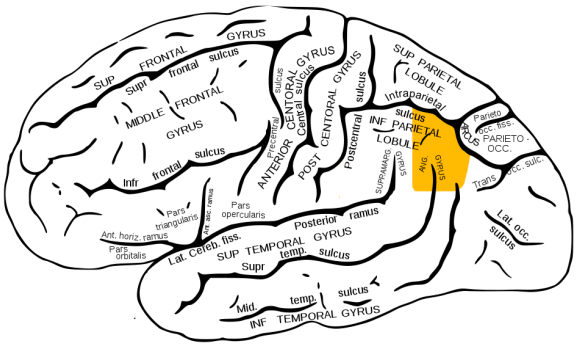

Fig. 6: Angular gyrus

- *Cuneus*: involved in basic visual processing
- *Precuneus*: involved in loads of stuff including default network and visuospatial processing
- *Superior temporal junction (temporoparietal junction)*: information processing and perception (right and left do not do exactly the same thing - right is more associated with attention and left with language processing)
- *Middle frontal gyrus*: part of prefrontal cortex - executive function including attention and working memory
- *Posterior cingulate*: central node in the resting state network
- *Superior temporal sulcus*: social perception - responds more to human stimuli rather than environmental ones
- *Inferior parietal lobe*: perception of emotions, faces, interpretation of sensory inputs

Regions marked with '*' surround the angular gyrus, which is a part fo the default state network.

A striking pattern of the data is the total dominance of the left primary auditory cortex (region 8) in as compared to the right primary auditory cortex (region 9) which hardly shows up at all. Many other symmetric regions seem to show up in pairs so this contrast is striking.

3) Looking for cyclic patterns: The lead matrix provides an insight into the temporal, cyclic behavior of the interrelated time series. The patterns of cyclic behavior that are observed universally, or which are prevalent in a population are of especial interest. To recover these data, we adapt an approach inspired by the *Hodge theory* paradigm [4]. If the global cycling in the activities of ROIs is present, but observed in noisy environments, then the recovery of this global cycle can be performed using the continuous relaxation to a one-dimensional cycle, fitting best with the observed cyclic orders in various triples of ROIs.

Each of the cyclic triples, after factoring out the cyclic symmetry, can appear in two versions, `ABC=BCA=CAB` or `ACB=CBA=BAC`.

Thus only the frequencies far away from 50% are informative. For the ROIs identified in the previous section, the frequencies (out of 200 subjects) are

(08,28,05)	127	(08,31,05)	130	(08,15,05)	127
(08,12,05)	123	(08,14,05)	127	(30,08,28)	133
(30,08,31)	129	(30,08,13)	120	(08,28,13)	122
(08,31,13)	125	(30,12,13)	133	(08,12,13)	137
(30,08,12)	124	(30,08,14)	123		

An MCMC search for the cyclic permutation of all 10 ROIs matching in an optimal way the observed triples resulted in the cyclic permutation (where the grouped ROIs are not separated significantly enough to impute an ordering within the group) shown on the Figure 7.

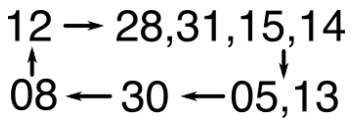

Fig. 7: Implied cycle of activity on ROIs with highest signal level.

Again, the left primary auditory cortex is a dominant ROI, represented in most of the triples. This results strongly suggest the triggering of what is assumed to be default network manifestations by an external stimulus.

Summarizing, our techniques allow to reveal patterns of cyclic behavior in the brain activities, which, however, challenge the assumption that they correspond to the resting state. This might have significant implications for the experimental procedures in the future.

VII. Conclusion

We proposed a novel, reparametrization invariant method of recovery of cyclic patterns in fMRI traces, and applied them to a widely used dataset of measurements.

References

[1] Yuliy Baryshnikov. Cyclicity and reparametrization-invariant features in time series. *Preprint*, 2016.

[2] Steven L Bressler and Vinod Menon. Large-scale brain networks in cognition: emerging methods and principles. *Trends in cognitive sciences*, 14(6):277–290, 2010.

[3] Kuo-Tsai Chen. Integration of paths–a faithful representation of paths by noncommutative formal power series. *Transactions of the American Mathematical Society*, pages 395–407, 1958.

[4] Jozef Dodziuk. Finite-difference approach to the hodge theory of harmonic forms. *American Journal of Mathematics*, 98(1):79–104, 1976.

[5] B Duplantier. Areas of planar brownian curves. *Journal of Physics A: Mathematical and General*, 22(15):3033, 1989.

[6] Manfred Eigen and Peter Schuster. A principle of natural self-organization. *Naturwissenschaften*, 64(11):541–565, 1977.

[7] Michael D Fox and Marcus E Raichle. Spontaneous fluctuations in brain activity observed with functional magnetic resonance imaging. *Nature Reviews Neuroscience*, 8(9):700–711, 2007.

[8] Karl J Friston. Functional and effective connectivity: a review. *Brain connectivity*, 1(1):13–36, 2011.

[9] R Matthew Hutchison, Thilo Womelsdorf, Elena A Allen, Peter A Bandettini, Vince D Calhoun, Maurizio Corbetta, Stefania Della Penna, Jeff H Duyn, Gary H Glover, Javier Gonzalez-Castillo, et al. Dynamic functional connectivity: promise, issues, and interpretations. *Neuroimage*, 80:360–378, 2013.